



Integrated Carbon Capture and Conversion: a review on C2+ product mechanisms and mechanism-guided strategies

February 2023

Changing the World's Energy Future

Asmita Jana, Ethan J. Crumlin, Jin Qian, Seth W Snyder



INL is a U.S. Department of Energy National Laboratory operated by Battelle Energy Alliance, LLC

DISCLAIMER

This information was prepared as an account of work sponsored by an agency of the U.S. Government. Neither the U.S. Government nor any agency thereof, nor any of their employees, makes any warranty, expressed or implied, or assumes any legal liability or responsibility for the accuracy, completeness, or usefulness, of any information, apparatus, product, or process disclosed, or represents that its use would not infringe privately owned rights. References herein to any specific commercial product, process, or service by trade name, trade mark, manufacturer, or otherwise, does not necessarily constitute or imply its endorsement, recommendation, or favoring by the U.S. Government or any agency thereof. The views and opinions of authors expressed herein do not necessarily state or reflect those of the U.S. Government or any agency thereof.

Integrated Carbon Capture and Conversion: a review on C₂+ product mechanisms and mechanism-guided strategies

Asmita Jana, Ethan J. Crumlin, Jin Qian, Seth W Snyder

February 2023

**Idaho National Laboratory
Idaho Falls, Idaho 83415**

<http://www.inl.gov>

**Prepared for the
U.S. Department of Energy
Under DOE Idaho Operations Office
Contract DE-AC07-05ID14517**

Integrated Carbon Capture and Conversion: a review on C₂₊ product mechanisms and mechanism-guided strategies

1 Asmita Jana^{1,2}, Seth W. Snyder³, Ethan J. Crumlin^{1,2*}, Jin Qian^{1*}

2 ¹ Chemical Science Division, Lawrence Berkeley National Laboratory, Berkeley, California 94720,
3 USA.

4 ² Advanced Light Source, Lawrence Berkeley National Laboratory, Berkeley, California 94720,
5 USA.

6 ³ Energy & Environment S&T, Idaho National Laboratory, Idaho Falls, Idaho 83415, USA.

7
8 *** Correspondence:**

9 Corresponding Author

10 ejcrumlin@lbl.gov, jqian2@lbl.gov

11 **Keywords: one-pot solution, carbon capture, carbon conversion, C₂₊ products, electrochemical**
12 **reduction, metal organic framework, copper catalysts**

13 Abstract

14 The need to reduce atmospheric CO₂ concentrations necessitates CO₂ capture technologies for
15 conversion into stable products or long-term storage. A single pot solution that simultaneously captures
16 and converts CO₂ could minimize additional costs and energy demands associated with CO₂ transport,
17 compression, and transient storage. While a variety of reduction products exist, currently, only
18 conversion to C₂₊ products including ethanol and ethylene are economically advantageous. Cu-based
19 catalysts have the best-known performance for CO₂ electroreduction to C₂₊ products. Metal Organic
20 Frameworks (MOFs) are touted for their carbon capture capacity. Thus, integrated Cu-based MOFs
21 could be an ideal candidate for the one-pot capture and conversion. In this paper, we review Cu-based
22 MOFs and MOF derivatives that have been used to synthesize C₂₊ products with the objective of
23 understanding the mechanisms that enable synergistic capture and conversion. Furthermore, we discuss
24 strategies based on the mechanistic insights that can be used to further enhance production. Finally, we
25 discuss some of the challenges hindering widespread use of Cu-based MOFs and MOF derivatives
26 along with possible solutions to overcome the challenges.

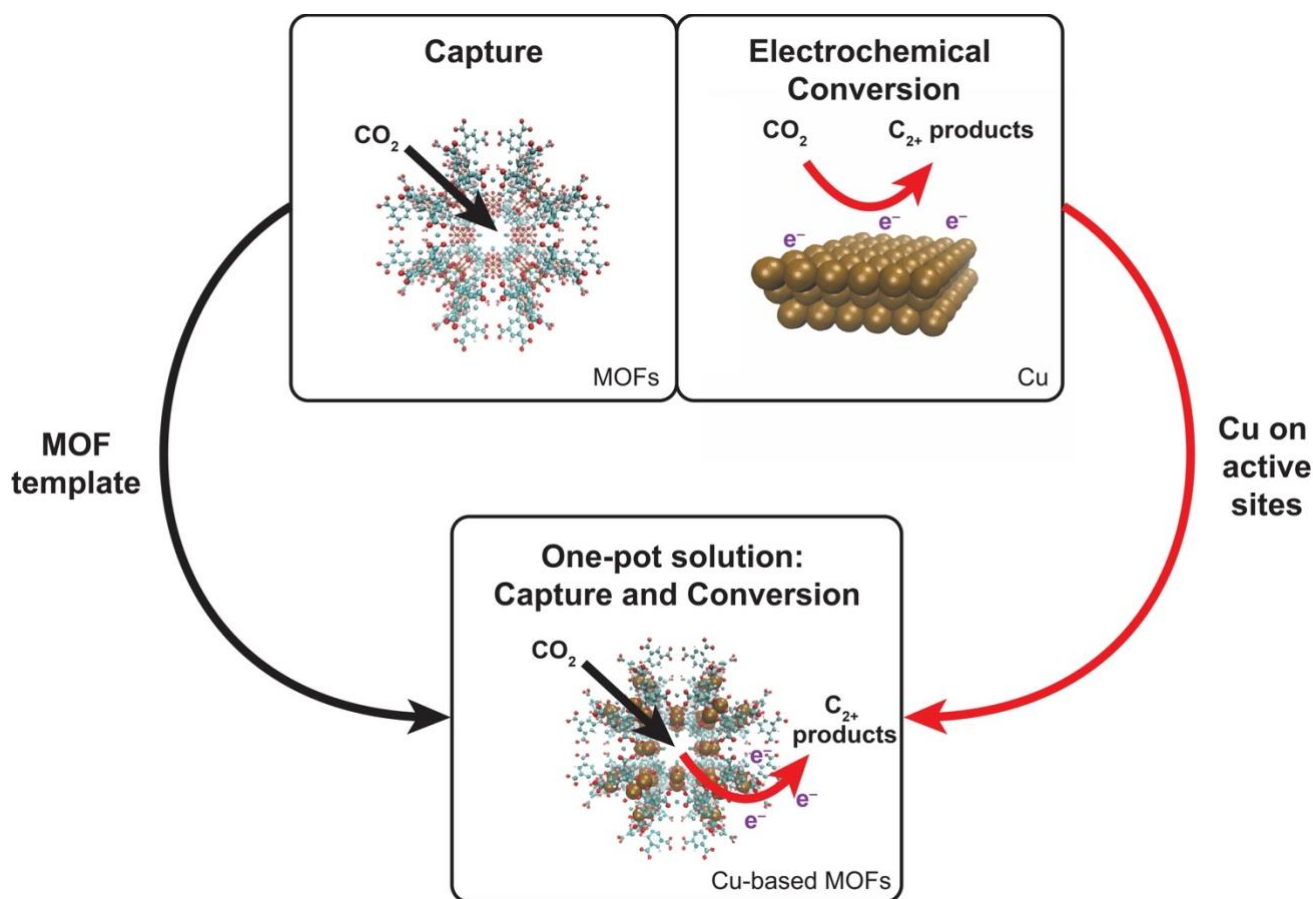


Figure TOC. A one-pot solution of combined capture and conversion represents the ideal solution with the MOFs component aiding capture and the Cu constituents supporting conversion to C_{2+} products via CO_2ER

1 Introduction

The exponential increase in greenhouse gases (GHGs) including CO_2 since the industrial revolution is the key driver of climate change (Field, Barros and on Climate Change, 2014; Sun *et al.*, 2017). Currently, the concentration of CO_2 in the atmosphere is greater than 400 ppm (Jiao *et al.*, 2019) with fossil fuels accounting for 75% of the increase in anthropogenic CO_2 emissions (Field, Barros and on Climate Change, 2014; Rafiee *et al.*, 2018). CO_2 levels are projected to increase to 685 ppm by 2050 (OECD, 2012) but CO_2 levels need to be maintained at ≤ 450 ppm to avoid seriously jeopardizing the environment (Metz and on Climate Change, 2007). While replacing fossil fuels with renewable sources of energy is the long-term solution, capturing CO_2 from concentrated sources and from the atmosphere is urgently needed (Birol, 2019; ‘Global Energy Transformation: A Roadmap to 2050’, 2018; Gielen *et al.*, 2019). Three main separation technologies to capture CO_2 are liquid absorbents, solid adsorbents, and membranes (‘Basic Research Needs for Carbon Capture: Beyond 2020: Report of the Basic Energy Sciences Workshop for Carbon Capture: Beyond 2020’, 2020) but the only method currently being used in an industrial scale is absorption using aqueous amine solutions (Iyer *et al.*, 2017). However, it is fraught with issues like solvent losses and comes with a high sorbent regeneration cost. Thus, there is an ongoing search for better materials (and processes) that can achieve efficient and cost-effective carbon capture (‘Basic Research Needs for Carbon Capture: Beyond 2020: Report of the Basic Energy

Sciences Workshop for Carbon Capture: Beyond 2020', 2020). In this review, we evaluate a class of solid adsorbents in more detail- Metal Organic Frameworks (MOFs). These crystalline porous materials are composed of multi-metallic units surrounded by organic linkers (Eddaoudi *et al.*, 2001; Long and Yaghi, 2009; Zhou *et al.*, 2012; “Joe” Zhou and Kitagawa, 2014; Lu *et al.*, 2014) and satisfy some of the prerequisites of an ideal CO₂ capture material: a. high selectivity towards binding CO₂, b. high capacity, c. low energy requirement for releasing CO₂, d. thermal and chemical stability along with thermal capacity, and e. good synthesizability.

The step following carbon capture is either storage or conversion. Limited known geological storage options along with associated costs of transportation and suffocation risks from potential leaks suggest that conversion and utilization should be strongly committed (Sabri *et al.*, 2021). Conversion achieves the dual objective of converting CO₂ to value-added products including urea, methane, methanol, etc., while simultaneously avoiding the risks associated with storage. Conversion of CO₂ invariably translates to CO₂ reduction. Most thermal CO₂ reduction requires harsh conditions involving high temperature and pressures, requires additional energy input and can hinder broad deployment. Depending on the energy source, it could require additional carbon-emitting fossil combustion. This can be circumvented by using CO₂ electrochemical reduction (CO₂ER) instead of thermal and pressure-driven methods (Kondratenko *et al.*, 2013; Lu *et al.*, 2014; Zhao *et al.*, 2017; Jiao *et al.*, 2019, Wang *et al.*, 2022). Electrochemistry enables production of chemicals that are often more difficult to produce from thermal methods (Gattrell, Gupta and Co, 2006; Kondratenko *et al.*, 2013). While a wide variety of value-added products can be obtained, not all of them are economically feasible. Nitopi *et al.* weighed the market price of an array of value-added products against the energy required to produce them and concluded that C₂₊ products such as ethanol, ethylene, and propanol are the most economically feasible (Nitopi *et al.*, 2019). Hence, in this review, we shall focus on processes that exclusively produce C₂₊ products. Among the catalysts used for CO₂ER, Cu-based ones are unparalleled for synthesis of C₂₊ products (Nitopi *et al.*, 2019).

In this review, we focus on the conversion part of the capture and conversion process because the former is a process driven by thermodynamics and is a very well-studied topic on its own (Eddaoudi *et al.*, 2001; Long and Yaghi, 2009; Zhou *et al.*, 2012; “Joe” Zhou and Kitagawa, 2014; Lu *et al.*, 2014). Here, we wanted to showcase the impact of electrocatalysis on CO₂ reduction within the framework of a conversion material. We explore mechanisms for CO₂ER to C₂₊ products in Cu-based electrodes to develop insights into the process. Such mechanistic knowledge shall guide different strategies that enhance C₂₊ product formation by optimizing the catalyst and reaction conditions. We then highlight the emerging potential of having a one-pot solution that combines capture and conversion. This has been demonstrated with Cu-based MOF derivatives where the constituent MOFs adsorb CO₂ and provide a nice framework for constituent Cu sites to act as catalytic sites for CO₂ER. Furthermore, the structure of MOF enhances catalytic activity via synergistic effects in addition to CO₂ capture. While some of the mechanistic insights and improvement strategies in Cu electrocatalysis are transferable, we also discuss the additional requirements that are mandated by the one-pot Cu-based MOF solution. Finally, we discuss challenges hindering commercial use of these materials and how they can be overcome, paving the way for using these materials as suitable candidates for broad deployment of CO₂ reduction systems.

2 CO₂ conversion

Catalysts used to fabricate electrodes are broadly classified into four groups based on the selectivity of their CO₂ reduction products: a. formate; b. CO; c. H₂; and d. hydrocarbon, aldehydes, and alcohols. The formate producers are metals such as Pb, Hg, Tl, and In, while some metals such as Au, Ag, and Zn primarily produce CO. A few metals including Ni, Fe, Pt, and Ti reduce water to H₂ and are termed H₂ producing. Cu is the only metal belonging to the fourth category making it ideal for producing C₂₊ products. This is heavily attributed to the unique characteristic of Cu of having a negative adsorption energy for CO while maintaining a positive one for H species. This translates to the ability to retain and eventually reduce CO while preventing the hydrogen evolution reaction (HER). The adsorption characteristics of CO play an instrumental role because reduction to CO is the first reaction step in CO₂ER to C₂₊ products (Nitopi *et al.*, 2019). CO production is enhanced in the presence of catalysts such as Ag and they have been increasingly used to design bi-metallic catalysts with increased reduction to C₂₊ products (Nitopi *et al.*, 2019).

While electrodes fabricated from Cu can synthesize a variety of products such as CO, formate, C₂H₄, and CH₄, we are primarily interested in producing C₂₊ products given their high benefit-to-cost ratio. In specific, formation of the C-C bond in C₂₊ is the critical first reaction for oligomerization into a range of materials, chemicals, and fuels, enabling CO₂ to serve as a primary industrial building block. Many processes exist to maximize the production of C₂₊ products but from a reduction pathway perspective, they broadly result in these effects: a. increasing the availability of CO and b. enhancing CO dimerization reactions. The first tier of products synthesized after two electron transfer from CO₂ in the CO₂ER reduction pathway consists of formate and CO (Nitopi *et al.*, 2019). The former is a terminal product, implying that it does not undergo further reduction. Thus, for C₂₊ production, we need to drive the reduction process to CO, not formate. Increasing the adsorption, transport, and overall availability of CO can enhance formation of C₂₊ products. This is the principle behind employing metals that selectively produce CO such as Ag, Au, and Zn as a co-catalyst (Nitopi *et al.*, 2019). For example, a study found Cu-Ag bimetallic electrodes resulted in higher production of CH₃CHO and C₂H₄ compared to pure Cu electrode (Ishimaru, Shiratsuchi and Nogami, 2000). The second process is based on a reaction pathway that involves enhancing CO dimerization reactions (Nitopi *et al.*, 2019). Cu (100) is observed to amplify those reactions and is reported to be one of the surfaces with a high selectivity for C₂H₄ over CH₄ (Hori *et al.*, 1995). There are other strategies to boost C₂₊ products, the most important and widespread one is increasing the electrochemically-active surface area (ECSA). Some methods for increasing ECSA include using Cu nanostructures and stepped Cu surfaces. For example, Manthiram *et al.* observed fourfold higher current density along with a faradaic efficiency of 80% for CH₄ production on Cu nanoparticles with an initial size of 7 nm as compared to polycrystalline Cu foil (Manthiram, Beberwyck and Alivisatos, 2014). These processes are depicted in **Figure 1**.

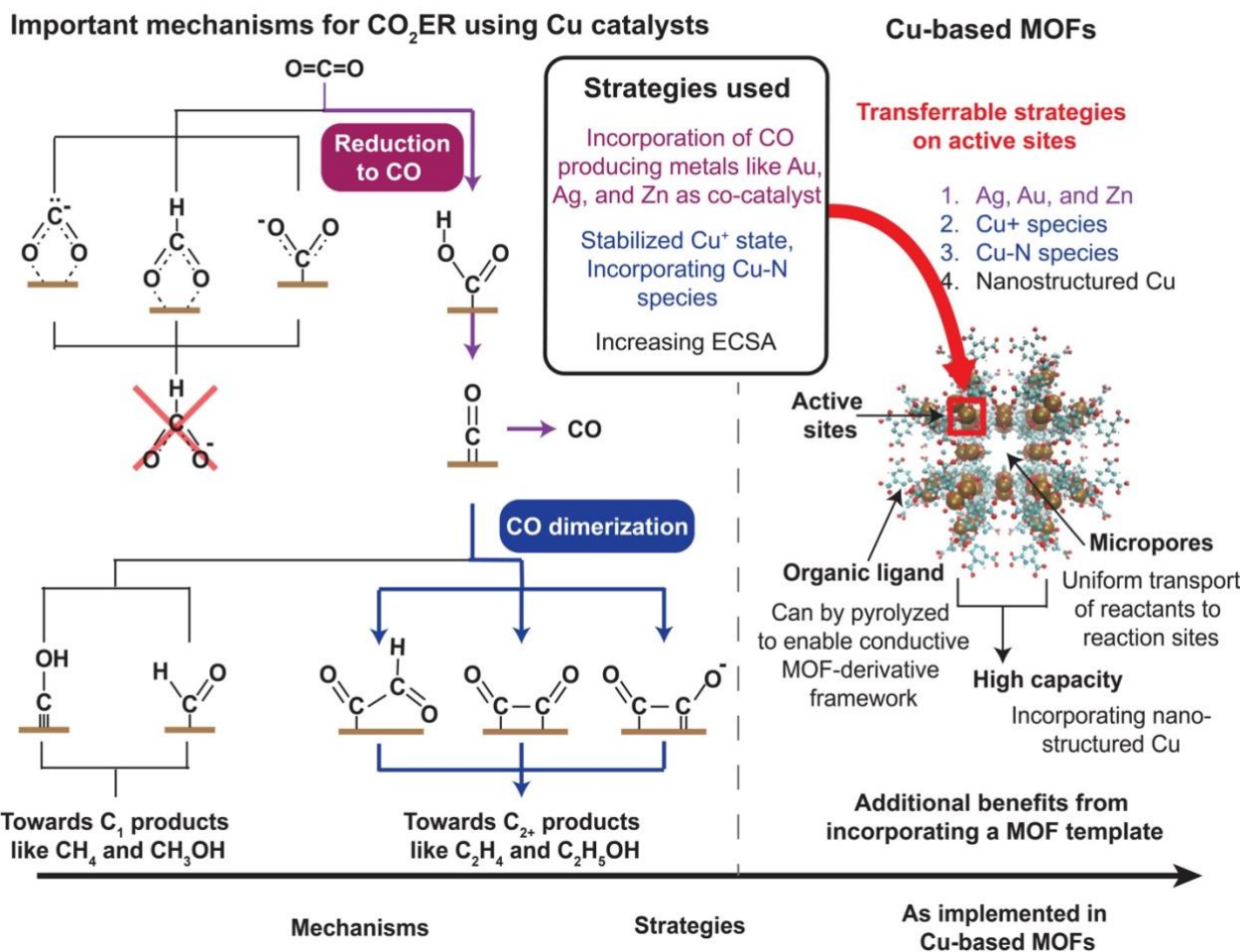


Figure 1. A partial CO₂ER pathway indicating major reactions process (Hori *et al.*, 1994, 1997; Peterson *et al.*, 2010; Kuhl *et al.*, 2012; Cheng, Xiao and Goddard, 2015; Kortlever *et al.*, 2015; Montoya *et al.*, 2015; Feaster *et al.*, 2017; Chernyshova, Somasundaran and Ponnuram, 2018; Garza, Bell and Head-Gordon, 2018; Lum *et al.*, 2018; Liu *et al.*, 2019; Nitopi *et al.*, 2019). Mechanisms that play a critical role in the production on C₂₊ products via CO₂ER on Cu-based catalysts along with strategies used to enhance them are specifically highlighted. These strategies can be implemented in a Cu-based MOF system; the chemically tunable active sites along with additional advantages of a MOF template for catalysis highlights the ability of Cu-based MOFs to produce C₂₊ products via CO₂ER

3 Integrated CO₂ capture and conversion

Carbon conversion is preceded by carbon capture, but such sequential treatment suffers from the additional cost required for compression and transportation. For transportation, CO₂ needs to be compressed up to 150 bar which translates to at least around 360 kJ/kg CO₂ of work (Huck *et al.*, 2014). Other challenges with compression include the removal of residual moisture to avoid creating corrosive conditions in the tank and dissipation of heat during the compression process. These costs can be avoided if both processes occur in the same plant location, termed an integrated cascade system (Sabri

et al., 2021). The extremely optimistic end of this spectrum is simultaneous capture and conversion. Often, this is achieved by materials that function as both CO₂ adsorbers and CO₂ reduction catalysts.

Interestingly, metal organic frameworks (MOFs) which belong to the category of solid adsorbers can serve as both an adsorbent for CO₂ capture as well as a catalyst for CO₂ conversion. Some of the attractive features of MOFs that make it ideal for CO₂ capture include a. porous structure, b. chemically tunability, c. compatibility with other materials, d. structural flexibility, and e. hydrophobicity (Ding *et al.*, 2019). The open metal sites and organic linkers serve as Lewis acid and basic sites, respectively, both of which can coordinate and bind CO₂ (Ding *et al.*, 2019). For example, M-MOF-74 (M: Mg, Ni, Co, Zn) coordinates CO₂ via the metal sites (Kong *et al.*, 2012; Queen *et al.*, 2014) while IRMOF uses its N-containing Lewis base (amines) as the site for binding CO₂ (Millward and Yaghi, 2005). Moreover, CO₂ capture is enhanced with linkers functionalized with polar functional groups like -F, -Br, -NO₂, and -SO₃ as the additional dipole interacts with the quadrupole of CO₂ (Debatin *et al.*, 2010; Gassensmith *et al.*, 2011; Zhang *et al.*, 2016; Mosca *et al.*, 2018; Ding *et al.*, 2019). Additionally, the chemical features can be altered by easily functionalizing the linkers and modifying metal centers. These sites and modifications enhance CO₂ capture via synergistic effects. Lastly, the pore size and flexibility of these hydrophobic structures are tunable (Ding *et al.*, 2019).

Synthesizing C₂₊ products via electroreduction of CO₂ calls for Cu-based electrodes to serve as catalysts. The easily tunable characteristic of MOFs translates to the ability to incorporate Cu within the framework (as shown in **Figure 1**). Cu-based MOFs such as HKUST-1 exist that exhibit selectivity for C₂₊ products when used as an electrochemical catalyst (Han *et al.*, 2021a). **Table 1** highlights the catalysts, products, and synthesis efficiency. More importantly, we believe that it is important to highlight that not only do Cu-based MOFs combine both capture and conversion capabilities, but the combination increases the performance of both processes.

First, the availability of uniformly dispersed active sites and high surface area already makes MOFs an excellent catalyst template in general while the constituent micropores ensure uniform transport of reactants to the catalytic sites (Ding *et al.*, 2019). MOFs have been used for thermal reduction of CO₂ to synthesize organic products via cycloaddition, carboxylation, and cyclization reactions (Zalomaeva *et al.*, 2013; Liu *et al.*, 2015; Zhang *et al.*, 2016; Liang *et al.*, 2017; Xiong *et al.*, 2017; Nguyen *et al.*, 2018; Wang *et al.*, 2018). For example, MMCF-2 has been shown to provide a 95% yield for cycloaddition of CO₂ with propylene oxide in the presence of a co-catalyst (Gao *et al.*, 2014).

Table 1: List of Cu-based materials used as electrodes for CO₂ER to C₂₊ products

Adsorber	Material category	Conductive component	Electrolyte	Reactor cell type	Potential (V vs SHE)	Potential (V vs RHE)	Products	Efficiency (%)	Current density (mA/cm ²)	Reference
Cu	Metal	Metal	0.1 M KHCO ₃	H-type pyrex cell	-1.44	-1.05	C ₂ H ₄	25.5	-5	(Hori <i>et al.</i> , 1995; Hori, 2008)
							C ₂ H ₅ OH	5.7		
							C ₃ H ₇ OH	3		
Cu (100)					-1.4	-1	C ₂ H ₄	40.4		
							Alcohol	12		
							Aldehyde	4.4		
Cu (110)					-1.55	-1.15	C ₂ H ₄	15.1		
							Alcohol	7.4		
							Aldehyde	3.1		
Cu (111)					-1.55	-1.15	C ₂ H ₄	8.3		
							Alcohol	3.3		
							Aldehyde	2.7		
Cu-BTC	MOF	Glassy carbon electrode	0.1 M KCl	Three electrode singles compartment electrochemical cell	-2.27		Oxalic acid	51	19.22	(Senthil Kumar, Senthil Kumar and Anbu Kulandainathan, 2012)
Cu-BTC			0.5 M KHCO ₃	Micro Flow cell, ElectroCell A/S	-0.28		C ₂ H ₅ OH	10.3	10	(Albo <i>et al.</i> , 2017)
HKUST-1		Carbon paper	0.1 M KHCO ₃	H-type cell		-0.98	C ₂ H ₄ , C ₂ H ₅ OH	58.6	19.2	(Han <i>et al.</i> , 2021)
MOF-Cu ₃ (HITP) ₂		Conducting support	0.1 M KHCO ₃	Two compartment H-cell	-1.56		C ₂ H ₄	48	48	(Sun <i>et al.</i> , 2021)
HKUST-1				Micro Flow cell, ElectroCell A/S			C ₂ H ₅ OH	15.9	10	(Albo <i>et al.</i> , 2017)
CuAdeAce								1.2		

CuDTA MOA								6		
CuZnDTA MOA								9.9		
Cs ⁺ modified Cu,Zn MOF (Zr ₁₂ BPDC)							C ₂ H ₅ OH			(An <i>et al.</i> , 2019)
Cu(II)/ade-MOF				H-type cell		-1.4	C ₂ H ₄	34	8.5	(Yang <i>et al.</i> , 2019)
MOF-Cu ₃ (HITP) ₂		Conducting support		H-cell, flow-cell			C ₂ H ₄	60-70		(Sun <i>et al.</i> , 2021)
OD Cu/C HKUST-1	MOF derivatives via pyrolysis	Carbonized structure	0.1 M KHCO ₃	Two bath cell		-0.1	C ₂ H ₅ OH	45.2-71.2		(Zhao <i>et al.</i> , 2017)
HKUST-1 with desymmetrized Cu dimer			1 M KOH	Flow cell	-1.07		C ₂ H ₄	45	262	(Nam <i>et al.</i> , 2018)
Cu MOF-NC; BEN-Cu BTC			0.1 M KHCO ₃	H-cell		-1.01	C ₂ H ₄	11.2	8	(Yao <i>et al.</i> , 2020)
							C ₂ H ₅ OH	18.4		
Cu@Cu _x O-MOF HKUST-1			0.1 M KHCO ₃	Flow cell		-1.58	C ₂ H ₄	51	150	(Yao <i>et al.</i> , 2020)
HKUST-MOF derived Cu _x O _y C _z			1M KOH	Three compartment cell			C ₂ H ₄ , C ₂ H ₆ , C ₂ H ₅ OH, C ₃ H ₇ OH	54	80	(Sikdar <i>et al.</i> , 2021)
CuZn-NC MOF-74			0.1 M KHCO ₃	H-type compression cell		-1	C ₂ H ₄ , C ₂ H ₅ OH	25	12	(Juntrapirom <i>et al.</i> , 2021)
Cu ₂ O/Cu@NC Cu-NBDC			0.1 M KHCO ₃			-1.6	C ₂ H ₄	23.9		(Jin <i>et al.</i> , 2021)
Cu-GNC-VL			0.5 M KHCO ₃	H-type cell		-0.87	C ₂ H ₅ OH	70.53	10.4	(Zhang <i>et al.</i> , 2020)
Ag/Cu on HKUST			1 M KOH	Three compartment glass cell		-0.28	C ₂ H ₄ , C ₂ H ₆ , C ₂ H ₅ OH, C ₃ H ₇ OH	21	120	(Sikdar <i>et al.</i> , 2022)
Cu/Cu ₂ O@NG (HKUST-1 and N-doped graphene)	MOF derivatives via electrochemical reaction	N-doped graphene	0.2 M KI	Single compartment gas diffusion cell		-1.9	C ₂ H ₄ , C ₂ H ₅ OH, C ₃ H ₇ OH	56	19	(Zhi <i>et al.</i> , 2021)
HKUST-1-derived Cu nanosheet		Cu foil	0.1 M KHCO ₃	H-type cell		-1.03	C ₂ products	56		(Wang <i>et al.</i> , 2021)

183

184 Second, nanostructured Cu has been shown to display a higher catalytic activity compared to its bulk
 185 counterpart owing to a higher ECSA (Nitopi *et al.*, 2019) arising from the structural increase in steps,
 186 facets, and edge atoms. Moreover, grain boundaries are found to promote C-C coupling reactions while
 187 suppressing HER (Sun *et al.*, 2021). This effect can be readily exploited in MOFs and they provide an
 188 opportunity of significantly enhancing ECSA by incorporating Cu nanostructures and single atoms.
 189 For example, Cu-based MOFs such as HKUST-1 have been shown to produce C₂H₄ and C₂H₅OH at
 190 59% efficiency (Han *et al.*, 2021a). Moreover, a Cu-based HKUST-1 embedded on carbon catalysts
 191 via an electrochemical reaction resulted in ~10-fold increase in faradaic efficiency for synthesizing C₂+
 192 products compared to a pristine Cu foil (Wang *et al.*, 2021). This enhancement was attributed to the
 193 stepped surfaces, facets, and edges that contributed to the 1.24-fold higher ECSA observed compared
 194 to the Cu foil. Cu nanocrystallites were generated in MOF-Cu₃(HITP)₂ and the rich grain boundaries
 195 aided in C-C coupling reactions resulting in producing C₂H₄ with 60-70% efficiency (Sun *et al.*, 2021).

196

197 Third and most importantly, MOFs provide a structure where additional chemical species can be easily
 198 incorporated among the plethora of active sites available. From studies done on Cu electrodes, a variety
 199 of additions were found to enhance CO₂ conversion that holds true for Cu-based MOFs as well, and
 200 are well-suited to be adapted within the MOF structure (**Figure 1**). One of the primary chemical
 201 modifications that enhances C₂+ product formation is the addition of metals that produce CO such as
 202 Au, Ag, and Zn as co-catalysts. As mentioned in section 1, Au nanoparticles dispersed on a
 203 polycrystalline Cu foil results in a 100x higher reduction rate to C₂+ products compared to Cu alone
 204 (Morales-Guio *et al.*, 2018). This effect is also observed in CuZn bimetallic material embedded in a
 205 carbonized MOF, where the influence of Zn led to a 5-fold increase in faradaic efficiency in producing
 206 C₂H₄ and C₂H₅OH (Juntrapirom *et al.*, 2021). A similar effect was also seen in Ag/Cu bimetallic
 207 catalysts based on a Cu-based MOF derivative where many C₂+ products were produced with an
 208 efficiency of 21% (Sikdar *et al.*, 2022).

209 MOFs can also incorporate non-metals within its framework. Appending N-containing Cu-N species
 210 is credited to amplify formation of C₂+ products and lend higher stability. The former is attributed to
 211 the more stable adsorption of the CH₂ intermediate species and inhibition of HER (Jin *et al.*, 2021).
 212 This is cited as the reason for the Cu₂O/Cu@NC catalyst made from Cu-NBDC MOF showing 24%
 213 efficiency in forming C₂H₄ in direct contrast to the Cu₂O/Cu@C catalyst (no N content) which did not
 214 produce any C₂H₄ (Jin *et al.*, 2021). N, N dimethylformamide (DMF) was used in Cu-BTC and it was
 215 found to increase dimerization reactions producing oxalic acid with an efficiency of 51% (Senthil
 216 Kumar, Senthil Kumar and Anbu Kulandainathan, 2012). Similarly, N-containing ligands in
 217 Cu(II)/ade-MOFs augmented C₂H₄ generation with a 45% efficiency (Yang *et al.*, 2019). An N-
 218 containing BEN-Cu-BTC derivative displayed efficiencies of 18% and 11% for C₂H₅OH and C₂H₄,
 219 respectively (Cheng *et al.*, 2019). As seen from section 2, adding N-containing species is also a strategy
 220 used to increase CO₂ capture as these groups interact with CO₂ to enhance adsorption making this a
 221 dual-purpose addition for both capture and conversion.

222

223 Furthermore, stabilizing the Cu⁺ state was shown to boost synthesis of C₂+ products via enhancing CO
 224 dimerization. This effect was observed in HKUST-1 where the high Cu⁺ /Cu⁰ ratio resulted in

producing C_2H_4 and C_2H_5OH with efficiency of 59% (Han *et al.*, 2021a). For similar reasons, the $Cu@Cu_xO$ structure in a Cu-based MOF derivative created C_2H_4 with 51% efficiency (Yao *et al.*, 2020).

While MOFs contain a plethora of advantages for CO_2ER , they are also plagued by some disadvantages. Some of them are the lack of conductivity and stability. This necessitates the addition of conductive supports that can in turn, complicate manufacturability. To truly enhance the catalytic activity to the maximum limit, we need to explore methods of making the MOF conductive on its own. Fortuitously, this can be achieved by pyrolyzing the MOFs to create MOF derivatives that not only are stable and conducting because of the carbonization of the organic linkers at high temperatures, but the process also creates additional active sites (Chen *et al.*, 2018). These reasons led to oxide-derived Cu/carbon catalyst generated from HKUST-1 via pyrolysis displaying a very low overpotential (-0.1 V vs RHE) for production of C_2H_5OH (Zhao *et al.*, 2017). Other such Cu-based MOF derivatives are listed in **Table 1** with the products and their efficiencies. These examples demonstrate that Cu-based MOF derivatives are well suited for CO_2ER to C_{2+} products.

4 Conclusion

An integrated carbon capture and conversion process is urgently needed to address atmospheric GHG concentrations. A one-pot solution avoids the additional cost, energy burden, and risks of compression and transportation that is associated with the CO_2 storage (and succeeding conversion). Only conversion to C_{2+} products is reported to be economically feasible. Since electrochemical reduction can be achieved under milder temperature and pressure conditions, they are preferred over thermal reduction. Cu-based catalysts are the gold standard for CO_2ER to synthesize C_{2+} products while MOFs are renowned for their CO_2 capture abilities. The chemical tunability of MOFs makes it possible to make Cu-based MOFs which fit perfectly with the requirement of the one-pot solution to enable CO_2 capture and CO_2ER synthesis of C_{2+} products. A series of Cu-based MOFs were explored and their performance in converting CO_2 to C_{2+} products were summarized (**Table 1**). We also delved deeper into the mechanisms that are involved in C_{2+} product formation and various strategies that can be used to enhance it. Notable among these processes are incorporating Ag/Au/Zn as co-catalysts to increase CO yield, as converting CO_2 to CO is the first step in the CO_2ER pathway. Another strategy is increasing the ECSA of the catalyst, which is the principle behind using nanostructured Cu instead of polycrystalline Cu foil. Moreover, these Cu nanoclusters can be embedded into MOFs as well. We also explored one critical disadvantage of MOFs for electrocatalysis: their low electrical conductivity, which necessitates using conductive supports. However, using pyrolyzed MOFs is an easy way to achieve the requisite electrical conductivity while also boosting stability. These materials classes are highlighted in **Figure 2**. We believe that this one-pot solution can be used for cleaned and reacted flue gas with the added advantage of avoiding energies involved in pressurization and collection. This has been reported in a few studies (D'Alessandro *et al.*, 2010; Kong *et al.*, 2012; McDonald *et al.*, 2012). Moreover, we want to highlight that this technology is in its conceptual stage and is not a working technology yet. Transformation to a full-fledged technology would require detailed evaluation of the scientific and engineering challenges such as separation of the reduction product from electrolyte and optimizing extended operation. A techno-economic analysis would be useful to determine the scalability and to direct the implementation towards viable pathways.

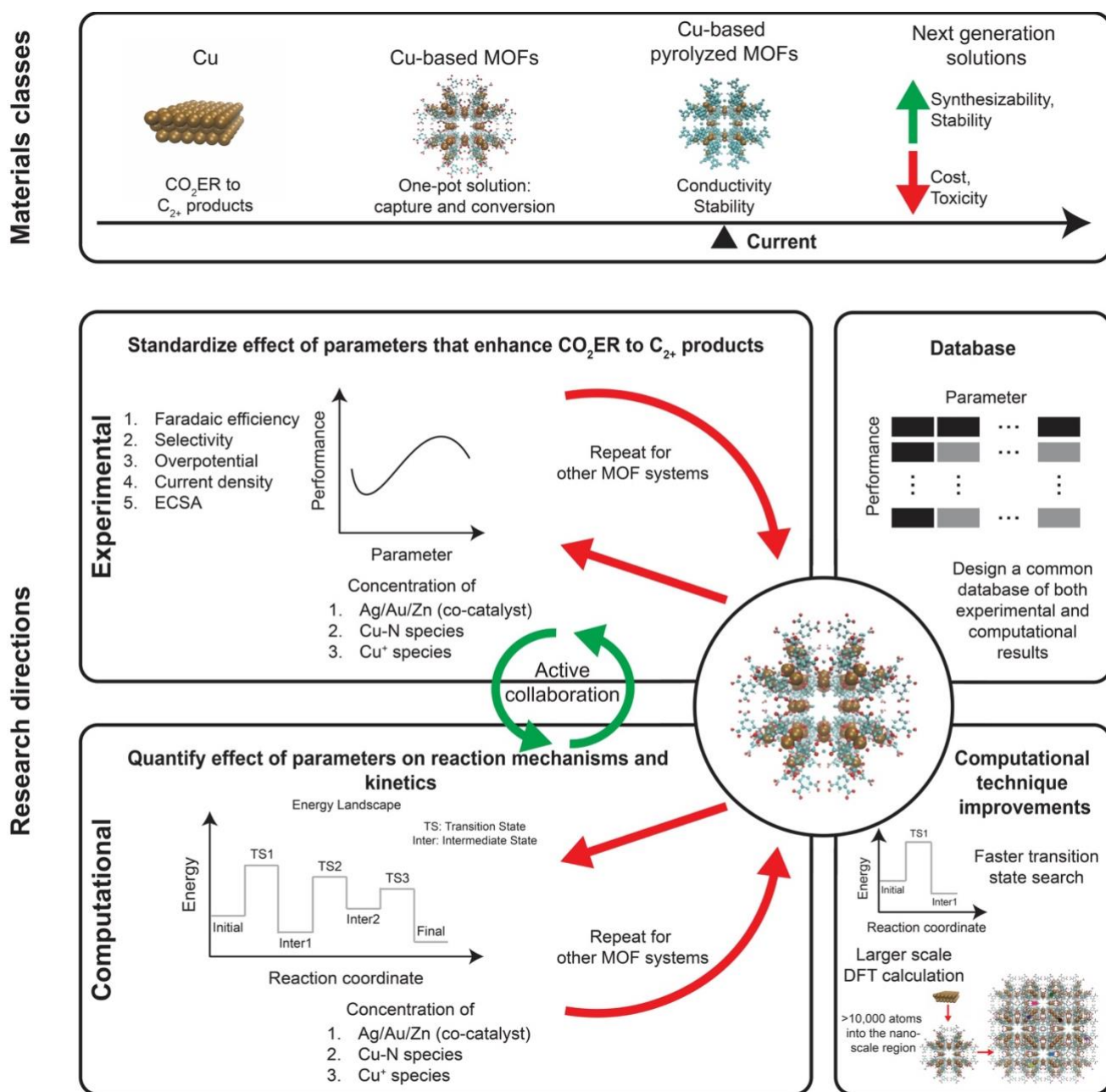


Figure 2. The materials classes involved in the CO₂ER to C₂₊ products: each successive progression highlights an improvement over the prior group. Future research directions are depicted.

While Cu-based MOFs display a high potential for CO₂ER, translating it to commercial use requires us to overcome challenges associated with the scaling-up of fabrication and deployment of MOFs. Firstly, MOFs are expensive and often, the primary contributing factor is the solvent cost (DeSantis *et al.*, 2017). For example, it accounts for 40% of the cost in HKUST-1 made via solvothermal process (DeSantis *et al.*, 2017). Opting for alternative processes such as liquid assisted grinding (LAG) and aqueous synthesis has the potential to reduce the cost by 34-83% as these processes use less solvent in comparison (DeSantis *et al.*, 2017). Moreover, the presence of inorganic nano-sized metal ions that are non-biodegradable along with trapped non-aqueous solvents such as dimethylformamide (DMF) make

MOFs toxic (Kumar *et al.*, 2019). More detailed studies on the toxic effects of MOFs are required for design of less toxic MOFs. Additionally, operation of MOFs for electrocatalytic applications often subject them to exposure to harsh chemical environments making chemical stability essential for efficient operation. Stability, in turn, is a direct result of the bonding environment including interactions such as hydrogen bonding and pi stacking (Coe, 2002; Nouar *et al.*, 2008; Howarth *et al.*, 2016). Incorporating a more inert central metal ion in the MOF structure can increase chemical stability (Kang *et al.*, 2011; Leus *et al.*, 2016). MOF derivatives synthesized via pyrolysis also slow down metal nanoparticle corrosion in the electrolyte, which in turn improves stability (Xiao, Wang and Guan, 2022). Another strategy to consider would be wrapping a protecting film on the surface of MOFs and MOF derivatives (Xiao, Wang and Guan, 2022). Mechanical stability is another factor affecting operation and while strategies like interweaving MOF networks (Tan and Cheetham, 2011; Burtch, Jasuja and Walton, 2014; Katz *et al.*, 2015) are often used, this can be redundant in MOFs for CO₂ER as liquid electrolyte filling MOFs enhances its stability already (Bennett *et al.*, 2015; van de Voorde *et al.*, 2015). Thermal stability is not as important in MOFs for CO₂ER as electroreduction does not require harsh thermal conditions for CO₂ capture or conversion. Finally, the poor electrical conductivity of the organic linkers necessitates presence of conductive substrates such as carbon cloth (Xiao, Wang and Guan, 2022). As previously highlighted, MOF derivatives created via pyrolysis can provide the required conductivity with the formed carbon layers. By altering synthesis parameters, the degree of graphitization can be enhanced. By adjusting the chemistry of the MOF precursors, the degree of defect carbon structure can be tuned. Both strategies can be used to optimize the resulting MOF derivative for enhanced conductivity (Xiao, Wang and Guan, 2022).

Lastly, we summarize our review with **Figure 2** and we provide conjectures regarding research needs for the next generation one-pot carbon-neutral solutions. Future research should standardize experimental results to facilitate comparison across multiple studies, enabling the community to accelerate the discovery process (Ward *et al.*, 2022). Most of the electrochemical reductions occur at the interface of the electrode and the electrolyte. Using experimental characterization techniques can help us understand bonding and identify species participating in the reaction. Overall, investigating the solid/liquid interface using characterization techniques requires overcoming two major challenges. First, characterization techniques need to be adapted for high pressure environments, as opposed to high vacuum, to replicate the more realistic experimental conditions. Second, the region corresponding to the electrical double layer is small and sandwiched between the bulk electrode and the bulk electrolyte, requiring for Å to nm resolution. Thus, the characterization techniques need to be specifically modified to enable a focus on the solid/liquid interface. Recent developments in characterization techniques like Fourier Transform Infrared spectroscopy (FTIR), Raman spectroscopy, and Ambient-Pressure X-Ray Spectroscopy (APXPS) have been able to overcome these challenges (Tian & Ren, 2004; Zaera, 2014; Favaro *et al.*, 2017b; Salmeron, 2018; Lu *et al.*, 2019; Han *et al.*, 2021b; Radjenovic *et al.*, 2021; Ye & Liu, 2021; Hao *et al.*, 2022). Using these characterization tools could enable a deeper understanding of the mechanisms involved in the activation process (Favaro *et al.*, 2017a; Qian *et al.*, 2019; Qian *et al.*, 2020). The field will benefit from active collaboration across experimental and computational investigations with the former focused on evaluating the performance of Cu-based MOFs as a function of parameters involved in the mechanism enhancement. On the other hand, computational studies can play a key role in assessing the energy landscape involved in the conversion of CO₂ to specific products. These assessments can be accelerated by implementing larger scale density functional theory (DFT) calculations (Kronik *et al.*, 2006; Zhou *et al.*, 2006; Xu *et al.*, 2019, 2021; Motamarri *et al.*, 2020; Dogan, Liou and Chelikowsky, 2022; Hao *et al.*, 2022; Xu, Prendergast and Qian, 2022) along with a faster transition state search procedure (Koistinen *et al.*, 2017; Garrido Torres *et al.*, 2019; Meyer, Schmuck and Hauser, 2019). Eventually, a database common

327 to both experimental and computational work, as outlined by the Materials Project (Jain *et al.*, 2013)
 328 can be constructed which can go a long way towards helping design high performance solutions.

329 **5 List of acronyms and abbreviations of MOFs**

DOBDC	2,5-Dihydroxyterephthalate
BTC	Benzene-1,3,5-tricarboxylate
BDC	1,4-Benzenedicarboxylate
BPDC	Biphenyl-1,4-dicarboxylate
M-MOF-74	[M ₂ (DOBDC)(H ₂ O) ₂] (M=Mg ²⁺ , Ni ²⁺ , Co ²⁺ , Zn ²⁺)
IRMOF-3	[Zn ₄ O(NH ₂ BDC) ₃]
HKUST-1	[Cu ₃ (BTC) ₂ (H ₂ O) ₃]
HITP	2,3,6,7,10,11-hexaiminotriphenylene
H-CuTCPP	Helical Cu porphyrinic MOF meso-tetra (4-carboxyphenyl) porphyrin
CuAdeAce	Copper(II)–adeninate–acetate
CuDTA MOA	Copper bis-bidentate dithiooxamidate metal-organic aerogel
Cu(II)/ade-MOF	CuII/adeninato/carboxylato metal-biomolecule frameworks
Cu MOF-NC; BEN-Cu BTC	Calcination of N-containing benzimidazole-modified Cu-BTC MOFs (BEN-Cu-BTC)
Cu-NBDC	Cu 2-aminoterephthalic acid
Cu-GNC-VL	Cu/Cu ₂ O nanocomposite loaded on the surface of carbon derived from direct carbonization of two-dimensional cross-like zeolitic imidazolate framework-L coated vertically on graphene oxide

H₄TACTMB

1,4,7,10-tetrazacyclododecane-
N,N',N'',N'''-tetra-p-methylbenzoic
acid

MMCF-2

[Cu₂(Cu-TACTMB)(H₂O)₃(NO₃)₂]

F-IRMOF-3

Functionalized IRMOF; NH₂ groups
converted to quaternary ammonium salt
through introduction of CH₃I

6 Conflict of Interest

The authors declare that the research was conducted in the absence of any commercial or financial relationships that could be construed as a potential conflict of interest.

7 Author Contributions

AJ and JQ contributed to the conception of the review. AJ wrote the first draft of the manuscript. All authors contributed to manuscript revision.

8 Funding

J.Q was supported by the Laboratory Directed Research and Development Program of Lawrence Berkeley National Laboratory through Contract No. DE-AC02-05CH11231. A. J. and E. J. C. were supported by an Early Career Award in the Condensed Phase and Interfacial Molecular Science Program, in the Chemical Sciences Geosciences and Biosciences Division of the Office of Basic Energy Sciences of the U.S. Department of Energy under Contract No. DE-AC02-05CH11231. SWS was supported by Idaho National Laboratory under the US Department of Energy through contract DE-AC07-05ID14517.

9 Acknowledgments

The authors are grateful to Dr. Yingchao Yang for his discussions and feedback.

10 References

Albo, J. *et al.* (2017) 'Copper-Based Metal–Organic Porous Materials for CO₂ Electrocatalytic Reduction to Alcohols', *ChemSusChem*, 10(6), pp. 1100–1109. Available at: <https://doi.org/10.1002/cssc.201600693>.

An, B. *et al.* (2019) 'Cooperative copper centres in a metal–organic framework for selective conversion of CO₂ to ethanol', *Nature Catalysis*, 2(8), pp. 709–717. Available at: <https://doi.org/10.1038/s41929-019-0308-5>.

355 'Basic Research Needs for Carbon Capture: Beyond 2020: Report of the Basic Energy Sciences
356 Workshop for Carbon Capture: Beyond 2020' (2020), p. 196.

357 Bennett, T.D. *et al.* (2015) 'Mechanical properties of zeolitic metal–organic frameworks:
358 mechanically flexible topologies and stabilization against structural collapse', *CrystEngComm*, 17(2),
359 pp. 286–289. Available at: <https://doi.org/10.1039/C4CE02145B>.

360 Birol, D.F. (2019) 'WORLD ENERGY OUTLOOK 2019', p. 810.

361 Burtch, N.C., Jasuja, H. and Walton, K.S. (2014) 'Water stability and adsorption in metal-organic
362 frameworks', *Chemical Reviews*, 114(20), pp. 10575–10612. Available at:
363 <https://doi.org/10.1021/cr5002589>.

364 Chen, Y.-Z. *et al.* (2018) 'Metal–organic framework-derived porous materials for catalysis',
365 *Coordination Chemistry Reviews*, 362, pp. 1–23. Available at:
366 <https://doi.org/10.1016/j.ccr.2018.02.008>.

367 Cheng, T., Xiao, H. and Goddard, W.A.I.I.I. (2015) 'Free-Energy Barriers and Reaction Mechanisms
368 for the Electrochemical Reduction of CO on the Cu(100) Surface, Including Multiple Layers of
369 Explicit Solvent at pH 0', *The Journal of Physical Chemistry Letters*, 6(23), pp. 4767–4773.
370 Available at: <https://doi.org/10.1021/acs.jpcclett.5b02247>.

371 Cheng, Y.-S. *et al.* (2019) 'An MOF-derived copper@nitrogen-doped carbon composite: the
372 synergistic effects of N-types and copper on selective CO₂ electroreduction', *Catalysis Science &*
373 *Technology*, 9(20), pp. 5668–5675. Available at: <https://doi.org/10.1039/C9CY01131E>.

374 Chernyshova, I. v, Somasundaran, P. and Ponnurangam, S. (2018) 'On the origin of the elusive first
375 intermediate of CO₂ electroreduction', *Proceedings of the National Academy of Sciences*, 115(40),
376 pp. E9261–E9270. Available at: <https://doi.org/10.1073/pnas.1802256115>.

377 Coe, C.G. (2002) 'Structural Effects on the Adsorptive Properties of Molecular Sieves for Air
378 Separation', in T.J. Pinnavaia and M.F. Thorpe (eds) *Access in Nanoporous Materials*. Boston, MA:
379 Springer US (Fundamental Materials Research), pp. 213–229. Available at: [https://doi.org/10.1007/0-](https://doi.org/10.1007/0-306-47066-7_14)
380 [306-47066-7_14](https://doi.org/10.1007/0-306-47066-7_14).

381 D'Alessandro, D. M., Smit, B., & Long, J. R. (2010) 'Carbon dioxide capture: prospects for new
382 materials', *Angewandte Chemie International Edition*, 49(35), 6058–6082. Available at
383 <https://doi.org/10.1002/anie.201000431>

384 Debatin, F. *et al.* (2010) 'In Situ Synthesis of an Imidazolate-4-amide-5-imidate Ligand and
385 Formation of a Microporous Zinc–Organic Framework with H₂-and CO₂-Storage Ability',
386 *Angewandte Chemie*, 122(7), pp. 1280–1284. Available at: <https://doi.org/10.1002/ange.200906188>.

387 DeSantis, D. *et al.* (2017) 'Techno-economic Analysis of Metal–Organic Frameworks for Hydrogen
388 and Natural Gas Storage', *Energy & Fuels*, 31(2), pp. 2024–2032. Available at:
389 <https://doi.org/10.1021/acs.energyfuels.6b02510>.

390 Ding, M. *et al.* (2019) 'Carbon capture and conversion using metal–organic frameworks and MOF-
391 based materials', *Chemical Society Reviews*, 48(10), pp. 2783–2828. Available at:
392 <https://doi.org/10.1039/C8CS00829A>.

393 Dogan, M., Liou, K.-H. and Chelikowsky, J.R. (2022) ‘Real-space Methods for Electronic Structure
394 Calculations of over 100,000 Atoms’. Available at: <https://doi.org/10.26153/TSW/43732>.

395 Eddaoudi, M. *et al.* (2001) ‘Modular Chemistry: Secondary Building Units as a Basis for the Design
396 of Highly Porous and Robust Metal–Organic Carboxylate Frameworks’, *Accounts of Chemical*
397 *Research*, 34(4), pp. 319–330. Available at: <https://doi.org/10.1021/ar000034b>.

398 Favaro, M. *et al.* (2017a) ‘Subsurface oxide plays a critical role in CO₂ activation by Cu (111)
399 surfaces to form chemisorbed CO₂, the first step in reduction of CO₂’, *Proceedings of the National*
400 *Academy of Sciences*, 114(26), 6706–6711. Available at: <https://doi.org/10.1073/pnas.1701405114>

401• Favaro, M. *et al.* (2017b) ‘Ambient-Pressure X-ray Photoelectron Spectroscopy to Characterize the
402 Solid/Liquid Interface: Probing the Electrochemical Double Layer’, *Synchrotron Radiation*
403 *News*, 30(2), 38–40. Available at: <https://doi.org/10.1080/08940886.2017.1289806>

405 Feaster, J.T. *et al.* (2017) ‘Understanding Selectivity for the Electrochemical Reduction of Carbon
406 Dioxide to Formic Acid and Carbon Monoxide on Metal Electrodes’, *ACS Catalysis*, 7(7), pp. 4822–
407 4827. Available at: <https://doi.org/10.1021/acscatal.7b00687>.

408 Field, C.B., Barros, V.R. and on Climate Change, I.P. (eds) (2014) *Climate change 2014: impacts,*
409 *adaptation, and vulnerability: Working Group II contribution to the fifth assessment report of the*
410 *Intergovernmental Panel on Climate Change*. New York, NY: Cambridge University Press.

411 Gao, W.-Y. *et al.* (2014) ‘Crystal Engineering of an nbo Topology Metal–Organic Framework for
412 Chemical Fixation of CO₂ under Ambient Conditions’, *Angewandte Chemie International Edition*,
413 53(10), pp. 2615–2619. Available at: <https://doi.org/10.1002/anie.201309778>.

414 Garrido Torres, J.A. *et al.* (2019) ‘Low-Scaling Algorithm for Nudged Elastic Band Calculations
415 Using a Surrogate Machine Learning Model’, *Physical Review Letters*, 122(15), p. 156001. Available
416 at: <https://doi.org/10.1103/PHYSREVLETT.122.156001/FIGURES/3/MEDIUM>.

417 Garza, A.J., Bell, A.T. and Head-Gordon, M. (2018) ‘Mechanism of CO₂ Reduction at Copper
418 Surfaces: Pathways to C₂ Products’, *ACS Catalysis*, 8(2), pp. 1490–1499. Available at:
419 <https://doi.org/10.1021/acscatal.7b03477>.

420 Gassensmith, J.J. *et al.* (2011) ‘Strong and Reversible Binding of Carbon Dioxide in a Green Metal–
421 Organic Framework’, *Journal of the American Chemical Society*, 133(39), pp. 15312–15315.
422 Available at: <https://doi.org/10.1021/ja206525x>.

423 Gattrell, M., Gupta, N. and Co, A. (2006) ‘A review of the aqueous electrochemical reduction of
424 CO₂ to hydrocarbons at copper’, *Journal of Electroanalytical Chemistry*, 594(1), pp. 1–19. Available
425 at: <https://doi.org/10.1016/j.jelechem.2006.05.013>.

426 Gielen, D. *et al.* (2019) ‘The role of renewable energy in the global energy transformation’, *Energy*
427 *Strategy Reviews*, 24, pp. 38–50. Available at: <https://doi.org/10.1016/j.esr.2019.01.006>.

428 ‘Global Energy Transformation: A Roadmap to 2050’ (2018), p. 76.

429 Han, Y. *et al.* (2021a) ‘Understanding Structure-activity Relationship on Metal-Organic-Framework-
 430 Derived Catalyst for CO₂ Electroreduction to C₂ Products’, *ChemElectroChem*, 8(16), pp. 3174–
 431 3180. Available at: <https://doi.org/10.1002/celec.202100942>.

432 Han, Y. *et al.* (2021b) ‘In situ characterization of catalysis and electrocatalysis using APXPS’, *ACS*
 433 *Catalysis*, 11(3), 1464–1484. Available at <https://doi.org/10.1021/acscatal.0c04251>

434 Hao, H. *et al.* (2022) ‘Chemical transformations and transport phenomena at interfaces’, *Wiley*
 435 *Interdisciplinary Reviews: Computational Molecular Science*, p. e1639. Available at:
 436 <https://doi.org/10.1002/WCMS.1639>.

437 Hori, Y. *et al.* (1994) ‘Electrocatalytic process of CO selectivity in electrochemical reduction of CO₂
 438 at metal electrodes in aqueous media’, *Electrochimica Acta*, 39(11), pp. 1833–1839. Available at:
 439 [https://doi.org/10.1016/0013-4686\(94\)85172-7](https://doi.org/10.1016/0013-4686(94)85172-7).

440 Hori, Y. *et al.* (1995) ‘Adsorption of CO accompanied with simultaneous charge transfer on copper
 441 single crystal electrodes related with electrochemical reduction of CO₂ to hydrocarbons’, *Surface*
 442 *Science*, 335, pp. 258–263. Available at: [https://doi.org/10.1016/0039-6028\(95\)00441-6](https://doi.org/10.1016/0039-6028(95)00441-6).

443 Hori, Y. *et al.* (1997) ‘Electrochemical Reduction of CO at a Copper Electrode’, *The Journal of*
 444 *Physical Chemistry B*, 101(36), pp. 7075–7081. Available at: <https://doi.org/10.1021/jp970284i>.

445 Hori, Y. (2008) ‘Electrochemical CO₂ Reduction on Metal Electrodes’, in C.G. Vayenas, R.E.
 446 White, and M.E. Gamboa-Aldeco (eds) *Modern Aspects of Electrochemistry*. New York, NY:
 447 Springer (Modern Aspects of Electrochemistry), pp. 89–189. Available at:
 448 https://doi.org/10.1007/978-0-387-49489-0_3.

449 Howarth, A.J. *et al.* (2016) ‘Chemical, thermal and mechanical stabilities of metal-organic
 450 frameworks’, *Nature Reviews Materials*, 1. Available at: <https://doi.org/10.1038/natrevmats.2015.18>.

451 Huck, J.M. *et al.* (2014) ‘Evaluating different classes of porous materials for carbon capture’, *Energy*
 452 *& Environmental Science*, 7(12), pp. 4132–4146. Available at: <https://doi.org/10.1039/C4EE02636E>.

453 Ishimaru, S., Shiratsuchi, R. and Nogami, G. (2000) ‘Pulsed Electroreduction of CO₂ on Cu-
 454 Ag Alloy Electrodes’, *Journal of The Electrochemical Society*, 147(5), p. 1864. Available at:
 455 <https://doi.org/10.1149/1.1393448>.

456 Iyer, S.S. *et al.* (2017) ‘Integrated Carbon Capture and Conversion To Produce Syngas: Novel
 457 Process Design, Intensification, and Optimization’, *Industrial & Engineering Chemistry Research*,
 458 56(30), pp. 8622–8648. Available at: <https://doi.org/10.1021/acs.iecr.7b01688>.

459 Jain, A. *et al.* (2013) ‘Commentary: The Materials Project: A materials genome approach to
 460 accelerating materials innovation’, *APL Materials*, 1(1), p. 011002. Available at:
 461 <https://doi.org/10.1063/1.4812323>.

462 Jiao, L. *et al.* (2019) ‘Toward CO₂ utilization for direct power generation using an integrated system
 463 consisting of CO₂ photoreduction with 3D TiO₂/Ni-foam and a photocatalytic fuel cell’, *Journal of*
 464 *Materials Chemistry A*, 7(11), pp. 6275–6284. Available at: <https://doi.org/10.1039/C8TA12255E>.

465 Jin, H. *et al.* (2021) ‘Cu-Based Catalyst Derived from Nitrogen-Containing Metal Organic
466 Frameworks for Electroreduction of CO₂’, *Wuli Huaxue Xuebao/ Acta Physico - Chimica Sinica*,
467 37(11). Available at: <https://doi.org/10.3866/PKU.WHXB202006017>.

468 “Joe” Zhou, H.-C. and Kitagawa, S. (2014) ‘Metal–Organic Frameworks (MOFs)’, *Chemical Society*
469 *Reviews*, 43(16), pp. 5415–5418. Available at: <https://doi.org/10.1039/C4CS90059F>.

470 Juntrapirom, S. *et al.* (2021) ‘Tuning CuZn interfaces in metal–organic framework-derived
471 electrocatalysts for enhancement of CO₂ conversion to C₂ products’, *Catalysis Science &*
472 *Technology*, 11(24), pp. 8065–8078. Available at: <https://doi.org/10.1039/D1CY01839F>.

473 Kang, I.J. *et al.* (2011) ‘Chemical and Thermal Stability of Isotypic Metal–Organic Frameworks:
474 Effect of Metal Ions’, *Chemistry – A European Journal*, 17(23), pp. 6437–6442. Available at:
475 <https://doi.org/10.1002/chem.201100316>.

476 Katz, M.J. *et al.* (2015) ‘Exploiting parameter space in MOFs: A 20-fold enhancement of phosphate-
477 ester hydrolysis with UiO-66-NH₂’, *Chemical Science*, 6(4), pp. 2286–2291. Available at:
478 <https://doi.org/10.1039/c4sc03613a>.

479 Koistinen, O.P. *et al.* (2017) ‘Nudged elastic band calculations accelerated with Gaussian process
480 regression’, *The Journal of Chemical Physics*, 147(15), p. 152720. Available at:
481 <https://doi.org/10.1063/1.4986787>.

482 Kondratenko, E. v *et al.* (2013) ‘Status and perspectives of CO₂ conversion into fuels and chemicals
483 by catalytic, photocatalytic and electrocatalytic processes’, *Energy & Environmental Science*, 6(11),
484 pp. 3112–3135. Available at: <https://doi.org/10.1039/C3EE41272E>.

485 Kong, X. *et al.* (2012) ‘CO₂ Dynamics in a Metal–Organic Framework with Open Metal Sites’,
486 *Journal of the American Chemical Society*, 134(35), pp. 14341–14344. Available at:
487 <https://doi.org/10.1021/ja306822p>.

488 Kortlever, R. *et al.* (2015) ‘Catalysts and Reaction Pathways for the Electrochemical Reduction of
489 Carbon Dioxide’, *The Journal of Physical Chemistry Letters*, 6(20), pp. 4073–4082. Available at:
490 <https://doi.org/10.1021/acs.jpcclett.5b01559>.

491 Kronik, L. *et al.* (2006) ‘PARSEC – the pseudopotential algorithm for real-space electronic structure
492 calculations: recent advances and novel applications to nano-structures’, *physica status solidi (b)*,
493 243(5), pp. 1063–1079. Available at: <https://doi.org/10.1002/PSSB.200541463>.

494 Kuhl, K.P. *et al.* (2012) ‘New insights into the electrochemical reduction of carbon dioxide on
495 metallic copper surfaces’, *Energy & Environmental Science*, 5(5), pp. 7050–7059. Available at:
496 <https://doi.org/10.1039/C2EE21234J>.

497 Kumar, P. *et al.* (2019) ‘Regeneration, degradation, and toxicity effect of MOFs: Opportunities and
498 challenges’, *Environmental Research*, 176, p. 108488. Available at:
499 <https://doi.org/10.1016/j.envres.2019.05.019>.

500 Leus, K. *et al.* (2016) ‘Systematic study of the chemical and hydrothermal stability of selected
501 “stable” Metal Organic Frameworks’, *Microporous and Mesoporous Materials*, 226, pp. 110–116.
502 Available at: <https://doi.org/10.1016/j.micromeso.2015.11.055>.

503 Liang, L. *et al.* (2017) ‘Carbon dioxide capture and conversion by an acid-base resistant metal-
 504 organic framework’, *Nature Communications*, 8(1), p. 1233. Available at:
 505 <https://doi.org/10.1038/s41467-017-01166-3>.

506 Liu, X. *et al.* (2019) ‘pH effects on the electrochemical reduction of CO(2) towards C2 products on
 507 stepped copper’, *Nature Communications*, 10(1), p. 32. Available at: [https://doi.org/10.1038/s41467-](https://doi.org/10.1038/s41467-018-07970-9)
 508 018-07970-9.

509 Liu, X.-H. *et al.* (2015) ‘An Efficient Nanoscale Heterogeneous Catalyst for the Capture and
 510 Conversion of Carbon Dioxide at Ambient Pressure’, *Angewandte Chemie International Edition*,
 511 54(3), pp. 988–991. Available at: <https://doi.org/10.1002/anie.201409103>.

512 Long, J.R. and Yaghi, O.M. (2009) ‘The pervasive chemistry of metal–organic frameworks’,
 513 *Chemical Society Reviews*, 38(5), pp. 1213–1214. Available at: <https://doi.org/10.1039/B903811F>.

514 Lu, W. *et al.* (2014) ‘Tuning the structure and function of metal–organic frameworks via linker
 515 design’, *Chem. Soc. Rev.*, 43(16), pp. 5561–5593. Available at: <https://doi.org/10.1039/C4CS00003J>.

516 Lu, Y. H. *et al.* (2019) ‘Infrared nanospectroscopy at the graphene–electrolyte interface’, *Nano*
 517 *letters*, 19(8), 5388–5393. Available at: <https://doi.org/10.1021/acs.nanolett.9b01897>

518 Lum, Y. *et al.* (2018) ‘Electrochemical CO Reduction Builds Solvent Water into Oxygenate
 519 Products’, *Journal of the American Chemical Society*, 140(30), pp. 9337–9340. Available at:
 520 <https://doi.org/10.1021/jacs.8b03986>.

521 Manthiram, K., Beberwyck, B.J. and Alivisatos, A.P. (2014) ‘Enhanced Electrochemical
 522 Methanation of Carbon Dioxide with a Dispersible Nanoscale Copper Catalyst’, *Journal of the*
 523 *American Chemical Society*, 136(38), pp. 13319–13325. Available at:
 524 <https://doi.org/10.1021/ja5065284>.

525 McDonald, T. M., Lee, W. R., Mason, J. A., Wiers, B. M., Hong, C. S., & Long, J. R. (2012).
 526 ‘Capture of carbon dioxide from air and flue gas in the alkylamine-appended metal–organic
 527 framework mmen-Mg₂ (dobpdc)’, *Journal of the American Chemical Society*, 134(16), 7056–7065.
 528 Available at: <https://doi.org/10.1021/ja300034j>
 529

530 Metz, B. and on Climate Change, I.P. (eds) (2007) *Climate change 2007: mitigation of climate*
 531 *change: contribution of Working Group III to the Fourth assessment report of the Intergovernmental*
 532 *Panel on Climate Change*. Cambridge ; New York: Cambridge University Press.

533 Meyer, R., Schmuck, K.S. and Hauser, A.W. (2019) ‘Machine Learning in Computational
 534 Chemistry: An Evaluation of Method Performance for Nudged Elastic Band Calculations’, *Journal of*
 535 *Chemical Theory and Computation*, pp. 6513–6523. Available at:
 536 https://doi.org/10.1021/ACS.JCTC.9B00708/ASSET/IMAGES/MEDIUM/CT9B00708_M018.GIF.

537 Millward, A.R. and Yaghi, O.M. (2005) ‘Metal–Organic Frameworks with Exceptionally High
 538 Capacity for Storage of Carbon Dioxide at Room Temperature’, *Journal of the American Chemical*
 539 *Society*, 127(51), pp. 17998–17999. Available at: <https://doi.org/10.1021/ja0570032>.

- 540 Montoya, J.H. *et al.* (2015) ‘Theoretical Insights into a CO Dimerization Mechanism in CO₂
541 Electroreduction’, *The Journal of Physical Chemistry Letters*, 6(11), pp. 2032–2037. Available at:
542 <https://doi.org/10.1021/acs.jpcllett.5b00722>.
- 543 Morales-Guio, C.G. *et al.* (2018) ‘Improved CO₂ reduction activity towards C₂+ alcohols on a
544 tandem gold on copper electrocatalyst’, *Nature Catalysis*, 1(10), pp. 764–771. Available at:
545 <https://doi.org/10.1038/s41929-018-0139-9>.
- 546 Mosca, N. *et al.* (2018) ‘Nitro-Functionalized Bis(pyrazolate) Metal–Organic Frameworks as Carbon
547 Dioxide Capture Materials under Ambient Conditions’, *Chemistry – A European Journal*, 24(50), pp.
548 13170–13180. Available at: <https://doi.org/10.1002/chem.201802240>.
- 549 Motamarri, P. *et al.* (2020) ‘DFT-FE – A massively parallel adaptive finite-element code for large-
550 scale density functional theory calculations’, *Computer Physics Communications*, 246, p. 106853.
551 Available at: <https://doi.org/10.1016/J.CPC.2019.07.016>.
- 552 Nam, D.-H. *et al.* (2018) ‘Metal–Organic Frameworks Mediate Cu Coordination for Selective CO₂
553 Electroreduction’, *Journal of the American Chemical Society*, 140(36), pp. 11378–11386. Available
554 at: <https://doi.org/10.1021/jacs.8b06407>.
- 555 Nguyen, P.T.K. *et al.* (2018) ‘New Metal–Organic Frameworks for Chemical Fixation of CO₂’, *ACS*
556 *Applied Materials & Interfaces*, 10(1), pp. 733–744. Available at:
557 <https://doi.org/10.1021/acsami.7b16163>.
- 558 Nitopi, S. *et al.* (2019) ‘Progress and Perspectives of Electrochemical CO₂ Reduction on Copper in
559 Aqueous Electrolyte’, *Chemical Reviews*, 119(12), pp. 7610–7672. Available at:
560 <https://doi.org/10.1021/acs.chemrev.8b00705>.
- 561 Nouar, F. *et al.* (2008) ‘Supramolecular building blocks (SBBs) for the design and synthesis of
562 highly porous metal-organic frameworks’, *Journal of the American Chemical Society*, 130(6), pp.
563 1833–1835. Available at: <https://doi.org/10.1021/ja710123s>.
- 564 OECD (2012) *OECD Environmental Outlook to 2050: The Consequences of Inaction*. Paris:
565 Organisation for Economic Co-operation and Development. Available at: https://www.oecd-ilibrary.org/environment/oecd-environmental-outlook-to-2050_9789264122246-en.
- 567 Peterson, A.A. *et al.* (2010) ‘How copper catalyzes the electroreduction of carbon dioxide into
568 hydrocarbon fuels’, *Energy & Environmental Science*, 3(9), p. 1311. Available at:
569 <https://doi.org/10.1039/c0ee00071j>.
- 570 Qian, J., *et al.* (2019) ‘Initial steps in forming the electrode–electrolyte interface: H₂O adsorption and
571 complex formation on the Ag (111) surface from combining quantum mechanics calculations and
572 ambient pressure X-ray photoelectron spectroscopy’, *Journal of the American Chemical*
573 *Society*, 141(17), 6946–6954. Available at <https://doi.org/10.1021/jacs.8b13672>
574
- 575 Qian, J. *et al.* (2020) ‘Addressing the sensitivity of signals from solid/liquid ambient pressure XPS
576 (APXPS) measurement’, *The Journal of chemical physics*, 153(4), 044709. Available at
577 <https://doi.org/10.1063/5.0006242>

578 Queen, W. *et al.* (2014) ‘Comprehensive study of carbon dioxide adsorption in the metal–organic
 579 frameworks M₂(dobdc) (M = Mg, Mn, Fe, Co, Ni, Cu, Zn)’, *Chemical Science*, 5(12), pp. 4569–
 580 4581. Available at: <https://doi.org/10.1039/C4SC02064B>.

581 Radjenovic, P. M. *et al.* (2021). Watching Reactions at Solid–Liquid Interfaces with in Situ Raman
 582 Spectroscopy. *The Journal of Physical Chemistry C*, 125(48), 26285–26295. Available at:
 583 <https://doi.org/10.1021/acs.jpcc.1c08640>

584 Rafiee, A. *et al.* (2018) ‘Trends in CO₂ conversion and utilization: A review from process systems
 585 perspective’, *Journal of Environmental Chemical Engineering*, 6(5), pp. 5771–5794. Available at:
 586 <https://doi.org/10.1016/j.jece.2018.08.065>.

587 Sabri, M.A. *et al.* (2021) ‘Current and future perspectives on catalytic-based integrated carbon
 588 capture and utilization’, *Science of The Total Environment*, 790, p. 148081. Available at:
 589 <https://doi.org/10.1016/j.scitotenv.2021.148081>.

590 Salmeron, M. (2018) ‘From surfaces to interfaces: ambient pressure XPS and beyond’, *Topics in*
 591 *Catalysis*, 61(20), 2044–2051. Available at: <https://doi.org/10.1007/s11244-018-1069-0>

592 Senthil Kumar, R., Senthil Kumar, S. and Anbu Kulandainathan, M. (2012) ‘Highly selective
 593 electrochemical reduction of carbon dioxide using Cu based metal organic framework as an
 594 electrocatalyst’, *Electrochemistry Communications*, 25, pp. 70–73. Available at:
 595 <https://doi.org/10.1016/j.elecom.2012.09.018>.

596 Sikdar, N. *et al.* (2021) ‘A Metal–Organic Framework derived Cu_xO_yC_z Catalyst for
 597 Electrochemical CO₂ Reduction and Impact of Local pH Change’, *Angewandte Chemie International*
 598 *Edition*, 60(43), pp. 23427–23434. Available at: <https://doi.org/10.1002/anie.202108313>.

599 Sikdar, N. *et al.* (2022) ‘Redox Replacement of Silver on MOF-Derived Cu/C Nanoparticles on Gas
 600 Diffusion Electrodes for Electrocatalytic CO₂ Reduction’, *Chemistry - A European Journal*, 28(12).
 601 Available at: <https://doi.org/10.1002/chem.202104249>.

602 Sun, H. *et al.* (2021) ‘Promoting ethylene production over a wide potential window on Cu crystallites
 603 induced and stabilized via current shock and charge delocalization’, *Nature Communications*, 12(1).
 604 Available at: <https://doi.org/10.1038/s41467-021-27169-9>.

605 Sun, K. *et al.* (2017) ‘Ultrahigh Mass Activity for Carbon Dioxide Reduction Enabled by Gold–Iron
 606 Core–Shell Nanoparticles’, *Journal of the American Chemical Society*, 139(44), pp. 15608–15611.
 607 Available at: <https://doi.org/10.1021/jacs.7b09251>.

608 Tan, J.C. and Cheetham, A.K. (2011) ‘Mechanical properties of hybrid inorganic–organic framework
 609 materials: establishing fundamental structure–property relationships’, *Chemical Society Reviews*,
 610 40(2), p. 1059. Available at: <https://doi.org/10.1039/c0cs00163e>.

611 Tian, Z. Q., & Ren, B. (2004) ‘Adsorption and reaction at electrochemical interfaces as probed by
 612 surface-enhanced Raman spectroscopy’, *Annu. Rev. Phys. Chem.*, 55, 197–229. Available at
 613 <https://doi.org/10.1146/annurev.physchem.54.011002.103833>

614 van de Voorde, B. *et al.* (2015) ‘Improving the mechanical stability of zirconium-based metal-
 615 organic frameworks by incorporation of acidic modulators’, *Journal of Materials Chemistry A*, 3(4),
 616 pp. 1737–1742. Available at: <https://doi.org/10.1039/c4ta06396a>.

- 617 Wang, D. *et al.* (2021) ‘HKUST-1-derived highly ordered Cu nanosheets with enriched edge sites,
618 stepped (211) surfaces and (200) facets for effective electrochemical CO₂ reduction’, *Chemosphere*,
619 278, p. 130408. Available at: <https://doi.org/10.1016/j.chemosphere.2021.130408>.
- 620 Wang, X. *et al.* (2018) ‘A metal–metalloporphyrin framework based on an octatopic porphyrin ligand
621 for chemical fixation of CO₂ with aziridines’, *Chemical Communications*, 54(10), pp. 1170–1173.
622 Available at: <https://doi.org/10.1039/C7CC08844B>.
- 623 Wang, Y. *et al.* (2022) ‘Catalytic Processes to Accelerate Decarbonization in a Net-Zero Carbon
624 World’, *ChemSusChem*, 15(24). Available at: <https://doi.org/10.1002/cssc.202201290>.
- 625 Ward, L. *et al.* (2022) ‘Principles of the Battery Data Genome’, *Joule*, 6(10), pp. 2253–2271.
626 Available at: <https://doi.org/10.1016/j.joule.2022.08.008>.
- 627 Xiao, L., Wang, Z. and Guan, J. (2022) ‘2D MOFs and their derivatives for electrocatalytic
628 applications: Recent advances and new challenges’, *Coordination Chemistry Reviews*, 472, p.
629 214777. Available at: <https://doi.org/10.1016/j.ccr.2022.214777>.
- 630 Xiong, G. *et al.* (2017) ‘Cluster-based MOFs with accelerated chemical conversion of CO₂ through
631 C–C bond formation’, *Chemical Communications*, 53(44), pp. 6013–6016. Available at:
632 <https://doi.org/10.1039/C7CC01136A>.
- 633 Xu, Q. *et al.* (2019) ‘Ab initio electronic structure calculations using a real-space Chebyshev-filtered
634 subspace iteration method’, *Journal of Physics: Condensed Matter*, 31(45), p. 455901. Available at:
635 <https://doi.org/10.1088/1361-648X/AB2A63>.
- 636 Xu, Q. *et al.* (2021) ‘SPARC: Simulation Package for Ab-initio Real-space Calculations’, *SoftwareX*,
637 15, p. 100709. Available at: <https://doi.org/10.1016/J.SOFTX.2021.100709>.
- 638 Xu, Q., Prendergast, D. and Qian, J. (2022) ‘Real-Space Pseudopotential Method for the Calculation
639 of 1 s Core-Level Binding Energies’, *Journal of Chemical Theory and Computation*, 18(9), pp.
640 5471–5478. Available at:
641 https://doi.org/10.1021/ACS.JCTC.2C00474/SUPPL_FILE/CT2C00474_SI_002.ZIP.
- 642 Yang, F. *et al.* (2019) ‘Highly efficient electroconversion of carbon dioxide into hydrocarbons by
643 cathodized copper–organic frameworks’, *Chemical Science*, 10(34), pp. 7975–7981. Available at:
644 <https://doi.org/10.1039/C9SC02605C>.
- 645 Yao, K. *et al.* (2020) ‘Metal–organic framework derived copper catalysts for CO₂ to ethylene
646 conversion’, *Journal of Materials Chemistry A*, 8(22), pp. 11117–11123. Available at:
647 <https://doi.org/10.1039/D0TA02395G>.
- 648 Ye, Y., & Liu, Z. (2021) ‘APXPS of Solid/Liquid Interfaces. In *Ambient Pressure Spectroscopy in*
649 *Complex Chemical Environments*’ (pp. 67–92). American Chemical Society. Available at
650 <https://doi.org/10.1021/bk-2021-1396.ch004>
651
- 652 Zaera, F. (2014) ‘New advances in the use of infrared absorption spectroscopy for the
653 characterization of heterogeneous catalytic reactions’ *Chemical Society Reviews*, 43(22), 7624–7663.
654 Available at: <https://doi.org/10.1039/C3CS60374A>

655 Zalomaeva, O. v *et al.* (2013) ‘Synthesis of cyclic carbonates from epoxides or olefins and CO₂
 656 catalyzed by metal-organic frameworks and quaternary ammonium salts’, *Journal of Energy*
 657 *Chemistry*, 22(1), pp. 130–135. Available at: [https://doi.org/10.1016/S2095-4956\(13\)60017-0](https://doi.org/10.1016/S2095-4956(13)60017-0).

658 Zhang, G. *et al.* (2016) ‘A Robust Sulfonate-Based Metal–Organic Framework with Permanent
 659 Porosity for Efficient CO₂ Capture and Conversion’, *Chemistry of Materials*, 28(17), pp. 6276–6281.
 660 Available at: <https://doi.org/10.1021/acs.chemmater.6b02511>.

661 Zhang, Yangyang *et al.* (2020) ‘Cu/Cu₂O Nanoparticles Supported on Vertically ZIF-L-Coated
 662 Nitrogen-Doped Graphene Nanosheets for Electroreduction of CO₂ to Ethanol’, *ACS Applied Nano*
 663 *Materials*, 3(1), pp. 257–263. Available at: <https://doi.org/10.1021/acsanm.9b01935>.

664 Zhao, K. *et al.* (2017) ‘CO₂ Electroreduction at Low Overpotential on Oxide-Derived Cu/Carbons
 665 Fabricated from Metal Organic Framework’, *ACS Applied Materials & Interfaces*, 9(6), pp. 5302–
 666 5311. Available at: <https://doi.org/10.1021/acsami.6b15402>.

667 Zhi, W.-Y. *et al.* (2021) ‘Efficient electroreduction of CO₂ to C₂–C₃ products on Cu/Cu₂O@N-
 668 doped graphene’, *Journal of CO₂ Utilization*, 50, p. 101594. Available at:
 669 <https://doi.org/10.1016/j.jcou.2021.101594>.

670 Zhou, X. *et al.* (2012) ‘Functionalized IRMOF-3 as efficient heterogeneous catalyst for the synthesis
 671 of cyclic carbonates’, *Journal of Molecular Catalysis A: Chemical*, 361–362, pp. 12–16. Available
 672 at: <https://doi.org/10.1016/j.molcata.2012.04.008>.

673 Zhou, Y. *et al.* (2006) ‘Parallel self-consistent-field calculations via Chebyshev-filtered subspace
 674 acceleration’, *Physical Review E - Statistical, Nonlinear, and Soft Matter Physics*, 74(6), p. 066704.
 675 Available at: <https://doi.org/10.1103/PHYSREVE.74.066704/FIGURES/3/MEDIUM>.

676

677

678

679

680

681